AIP Advances

Electron transfer characteristics of amino acid adsorption on epitaxial graphene FETs on SiC substrates

Cite as: AIP Advances **12**, 105310 (2022); https://doi.org/10.1063/5.0124084
Submitted: 02 September 2022 • Accepted: 19 September 2022 • Published Online: 18 October 2022

Sota Yamasaki, Hiroki Nakai, Keita Murayama, et al.

Electron transfer characteristics of amino acid adsorption on epitaxial graphene FETs on SiC substrates

Cite as: AIP Advances 12, 105310 (2022); doi: 10.1063/5.0124084
Submitted: 2 September 2022 • Accepted: 19 September 2022 •
Published Online: 18 October 2022

Sota Yamasaki,[1] Hiroki Nakai,[1] Keita Murayama,[1] Yasuhide Ohno,[2,a)] and Masao Nagase[2]

AFFILIATIONS

[1] Graduate School of Advanced Technology and Science, Tokushima University, 2-1 Minamijyousanjima, Tokushima 770-8506, Japan
[2] Institute of Post LED Photonics, Tokushima University, 2-1 Minamijyousanjima, Tokushima 770-8506, Japan

[a)] **Author to whom correspondence should be addressed:** ohno@ee.tokushima-u.ac.jp

ABSTRACT

Clarifying the adsorption characteristics of biomolecules on graphene surfaces is critical for the development of field-effect transistor (FET)-based biosensors for detecting pH, DNA, proteins, and other biomarkers. Although there are many reports on biomolecule detection using graphene FETs, the detection mechanism has not yet been clarified. In this study, the adsorption behavior and electron transfer characteristics of 20 proteinogenic amino acids on graphene field-effect transistors are investigated. Large single-crystal graphene films were epitaxially grown on SiC substrates by a resist-free metal stencil mask lithography process then patterned by air plasma etching to form FET devices. Amino acids with different charge conditions (positive or negative charge) were introduced onto the epitaxial graphene surface in solution. The charge neutral points of the drain current vs gate voltage curves shifted in the negative gate voltage direction after the introduction of all amino acids, regardless of the type of amino acid and its charge condition. These amino acid adsorption characteristics agree well with previously reported protein adsorption characteristics on epitaxial graphene surfaces, indicating that the adsorption of proteins in the liquid phase occurs by electron doping to the graphene surface. These results indicate that non-specific protein binding always leads to electron doping of epitaxial graphene FETs.

Field-effect transistor (FET)-based biosensing devices are promising for clinical diagnostics, point-of-care testing, and on-site sensing applications owing to their ability to instantaneously measure even small amounts of analytes with high sensitivity.[1,2] FET-based biosensors for the detection of pH, DNA, proteins, and other biomarkers have been developed from nanomaterials such as silicon nanowires,[3,4] carbon nanotubes,[5,6] and monolayer MoS_2 films.[7] Graphene is an attractive two-dimensional material for FET-based biosensors owing to its high carrier mobility, chemical stability, and large specific surface area, among other excellent properties.[8–13]

For the practical application of graphene FET-based biosensors, it is necessary to characterize the electrical changes that occur during both specific binding of the biomolecule to the receptor of interest and non-specific binding of the biomolecule to the FET channel. In particular, clarifying the adsorption characteristics of biomolecules on graphene surfaces is of particular significance for functionalizing the graphene surface and improving the signal to noise ratio. Moreover, although there are many reports on biomolecule detection using graphene FETs, the detection mechanism has not yet been clarified. For example, the direction in which the transfer characteristics shift sometimes differs, even for the same protein.[14,15] A key limitation to these investigations is that graphene films are commonly grown by chemical vapor deposition, which produces polycrystalline films. These films are then transferred to an insulating substrate, such as SiO_2, for device fabrication, which can introduce contamination, defects, and dislocations.[5,16–19] These factors affect the transfer characteristics of graphene-based biosensors. Therefore, it is necessary to use a transfer-free and resist-free method to fabricate single-crystal

graphene FETs to investigate their inherent sensing and adsorption characteristics.

Epitaxial graphene films synthesized on semi-insulating 4H–SiC substrates form large-area single crystals without a transfer process.[20,21] Therefore, these films could be used to investigate the inherent sensing and adsorption characteristics of graphene-based FETs, since other factors, such as defects, dislocations, polymer contamination, and ionic impurities, can be neglected. Recently, the ion sensitivity and protein adsorption properties of epitaxial graphene FETs have been investigated, and the results showed that ions do not adsorb onto the basal plane of the epitaxial graphene surface and many proteins donate electrons to the epitaxial graphene surface, which is independent of charge state, isoelectric point (pI), and pH.[22,23] However, the detailed mechanism of charge transfer during protein adsorption has not been clarified. Proteins have heterogeneous shapes and properties, and various factors, such as hydrogen bonding, electrostatic interactions, hydrophobic interactions, and van der Waals forces with other molecules, affect their adsorption behavior.[24,25] Since proteins comprise assemblies of up to 20 different amino acids, investigating the adsorption properties of these amino acids on graphene surfaces can provide detailed insight into the protein detection mechanism of graphene FET-based biosensors. Molecular adsorption on graphene and carbon nanotubes has been intensively studied,[26–28] and several researchers have performed theoretical calculations on the adsorption of amino acids on graphene.[29–32] However, most of them only considered adsorption in the gas phase partly because there are limited experimental data on the results in liquids. Furthermore, the adsorption of amino acids on graphene surfaces has not been experimentally studied yet because most experiments have used silicon or silica surfaces.[33–35] Therefore, in this study, we measured the adsorption behavior of 20 proteinogenic amino acids on epitaxial graphene FETs. The FET devices were fabricated by a resist-free metal stencil mask lithography method.

Single-crystal graphene films were grown on 10 × 10 mm^2 semi-insulating 4H–SiC (0001) substrates (Cree Inc.). The substrate was placed in a rapid thermal annealer (SR1800, Thermo Riko, Japan) and annealed at 1620 °C for 5 min in an Ar atmosphere at 100 Torr. The average sheet resistance, electron mobility, and carrier density of the graphene films were measured by the van der Pauw method to be 876 Ω/sq., 1075 $cm^2/(V\,s)$, and 6.6 × 10^{12} cm^{-2}, respectively. These values indicate that the single-crystal graphene films were of high quality.[20] The electron mobility of the epitaxial graphene film showed rather small because of the high electron concentration. However, the electron mobility showed more than 10 000 $cm^2/(V\,s)$ for a top-gated operation.[36] Raman spectra of the epitaxial graphene film are shown in the supplementary material. Figure 1 shows a schematic of the measurement setup using an epitaxial graphene FET. A six-terminal hole bar pattern was formed by metal stencil mask lithography on the epitaxial graphene film on the SiC substrate for electrical measurements without contact resistance. The metal mask was cleaned by ultrasonic cleaning using ethanol and ultrapure water, and then placed on the graphene film without gaps. The graphene film was patterned by air plasma etching. The size of the channel was 3 × 3 mm^2. Gold foils were placed at the edges of the device to prevent leakage current from the metal to the solution during the measurement and the electrical properties were measured by a four-probe method, which is impervious to the contact resistance between the graphene and gold foils. A silicone rubber container was placed on the graphene channel. An Ag/AgCl reference electrode was used as the top-gate electrode. All amino acids were purchased from Merck KGaA.

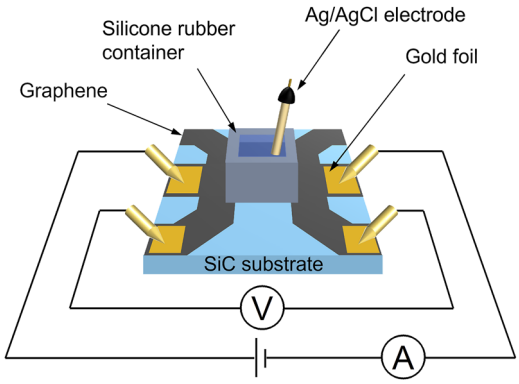

FIG. 1. Schematic of experimental setup using the epitaxial graphene FET. 10 × 10 mm^2 epitaxial graphene films were patterned to channel sizes of 3 × 3 mm^2.

Two kinds of pH-adjusted buffer solution were prepared. First, a 10 mM acetate buffer solution (ABS) was prepared by combining acetic acid and sodium acetate. Second, a 10 mM phosphorus buffer solution (PBS) was prepared by combining sodium dihydrogen phosphate dihydrate and disodium hydrogen phosphate dodecahydrate. The pH of these buffer solutions was adjusted from 4.0 to 5.5 and 6.0 to 8.0, respectively, by changing the ratio of the constituent compounds. The pH of each buffer solution was measured using a pH meter (F-71, Horiba, Ltd.). Proteinogenic amino acids were dissolved in the buffer solution at concentrations of 1 pM–100 μM. To measure the electrical properties of the graphene FET in contact with the amino-acid-containing buffer solutions, the solution was poured into the silicone rubber container on the graphene FET channel. The Ag/AgCl reference electrode was placed in the solution to apply the gate voltage, and the electrical characteristics were measured using a semiconductor parameter analyzer (B1500A, Keysight Technologies, USA). We focused only on the shift of the charge neutral point of the top-gate voltage, which is a typical parameter for molecular detection using graphene FETs.[23,37–39]

Figure 2 shows the transfer characteristics (drain current I_D vs gate voltage V_G) of the graphene FET in contact with L-asparagine monohydrate (Asn)-containing ABS [pH 4.4; Fig. 2(a)] and PBS [pH 7.4; Fig. 2(b)] at different Asn concentrations. The pI of Asn is 5.41; hence, Asn was positively and negatively charged in ABS and PBS, respectively. Figures 2(a) and 2(b) show that, as Asn was added to the solution, the I_D–V_G characteristics of the graphene FET shifted in the negative gate voltage direction, regardless of the whether Asn had a positive or negative charge. As the Asn concentration increased, the size of the shift increased until an approximately stable charge neutral point was reached.

To clarify the origin of the I_D–V_G shift, the charge neutral point shift was plotted as a function of the Asn concentration, as

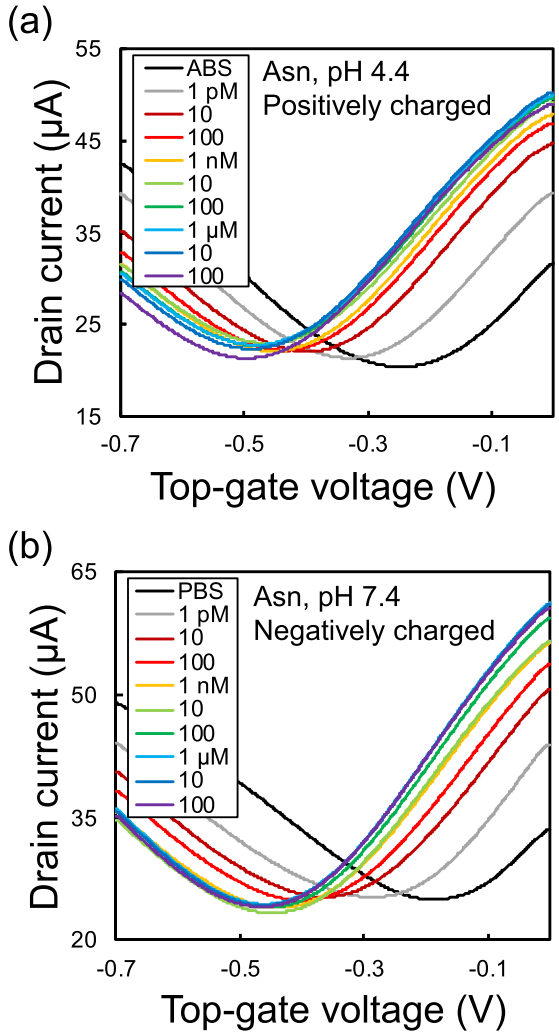

FIG. 2. I_D–V_G characteristics of the graphene FET with Asn adsorption at various concentrations: (a) pH 4.4 and (b) 7.4.

shown in Fig. 3. The negative voltage shift for both positively and negatively charged Asn increased rapidly at low concentrations and saturated at high concentrations. The plots were fitted by the Sips (Langmuir–Freundlich) model to confirm whether the origin of the shift was the adsorption of the amino acid onto the epitaxial graphene surface[40,41]

$$\Delta V = \Delta V_{\max} \frac{(C/K_D)^a}{1 + (C/K_D)^a}, \quad (1)$$

where ΔV, $\Delta V_{\max}$, C, and K_D are the charge neutral point shift, maximum charge neutral point shift when all channel surfaces are occupied by amino acids, concentration of the buffer solution, and equilibrium dissociation constant, respectively. α is an exponent with a value of between 0 and 1. The best fit for both positive and negative data resulted in parameter values of $\Delta V_{\max} = -0.275$ V, $K_D = 3.8$ pM, α = 0.42 and $\Delta V_{\max} = -0.247$ V, $K_D = 5.8$ pM, α = 0.33,

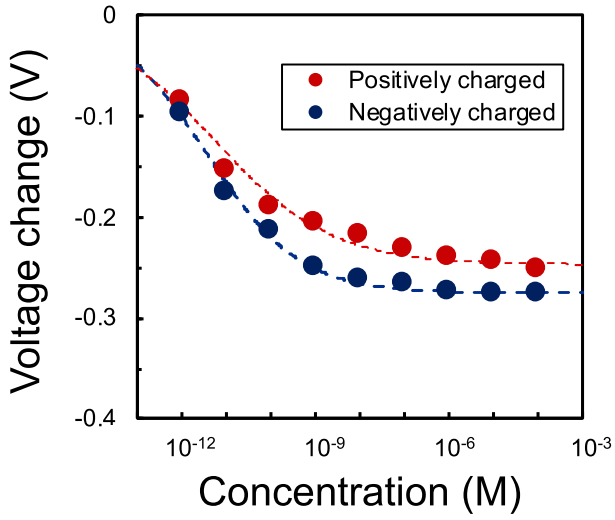

FIG. 3. Net voltage shift plotted as a function of Asn concentration. Red and blue dashed lines are Sips model fitting lines.

respectively. The red and blue dashed lines in Fig. 3 are the fitting curves for positively and negatively charged Asn solutions, respectively. The trend of the voltage shift fitted well with the Sips model in both cases, indicating that amino acid adsorption is the cause of the I_D–V_G shift.

The adsorption characteristics of the 19 other proteinogenic amino acids are shown in the supplementary material. The proteinogenic amino acids were categorized into six groups, namely, polar, nonpolar, aromatic, sulfur-containing, acidic, and basic, according to the nature of their side chains. Figure 4 shows the I_D–V_G shifts of representative amino acids in each of these categories

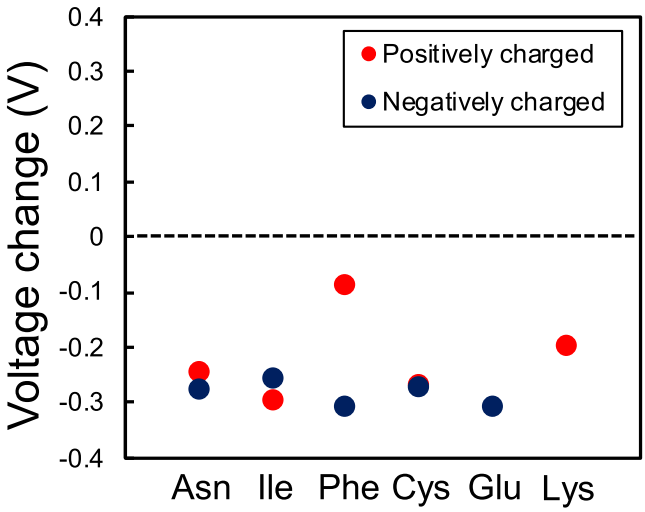

FIG. 4. I_D–V_G characteristic shifts for representative polar (Asn), nonpolar (Ile), aromatic (Phe), sulfur-containing (Cys), acidic (Glu), and basic (Lys) amino acids (classified according to the nature of their side chains).

(Asn, L-isoleucine (Ile), L-phenylalanine (Phe), L-cysteine (Cys), L-glutamic acid (Glu), and L-lysine (Lys), respectively). The pI values of the acidic (Glu) and basic (Lys) amino acids are too low (3.2) and too high (9.6), respectively, to prepare positively and negatively charged solutions, respectively. Therefore, only one charge is shown for these amino acids. For all six amino acids in Fig. 4, the charge neutral point of the epitaxial graphene FET shifted in the negative direction upon adsorption, regardless of whether the charge of the amino acid was positive or negative. This indicates that amino acid adsorption causes electron doping of the graphene film, independently of the structure and properties of the amino acid. A negative charge neutral point shift was observed for all 20 of the proteinogenic amino acids, indicating that all proteinogenic amino acids induce electron doping of epitaxial graphene films when adsorbed onto their surface. Notably, these amino acid adsorption characteristics explain the adsorption characteristics of proteins, which also cause electron doping of graphene films.[23]

Previous experiments on the ion sensitivity of epitaxial graphene FETs have demonstrated that phthalic acid ions cause specific I_D–V_G shifts, indicating that the π-orbitals of aromatic rings bind to the graphene surface by π–π interactions, leading to electron doping of the epitaxial graphene film.[22] Therefore, it is necessary to distinguish between the effect of π–π interactions and electron transfer. Qin *et al.*[42] performed density functional theory (DFT) molecular simulations of the interaction between L-leucine (Leu) and graphene surfaces. They found that the electronic structure of graphene can be controlled by the orientation of Leu. In general, the adsorption direction is expected to change depending on whether the adsorbed amino acid has a positive or negative charge. On the other hand, if the amino acid adsorbs on graphene via π–π interactions, as is expected for aromatic amino acids, the adsorption direction is unlikely to change with the charge state. Herein, although the adsorption direction did not change, the size of the charge neutral point shift was very different depending on the charge state. Therefore, it is possible that the charge state affects the size of the charge neutral point shift. Further investigations are needed to clarify why different I_D–V_G shifts were observed.

In summary, we investigated the adsorption characteristics of 20 types of proteinogenic amino acids in solution on epitaxial graphene FETs on SiC substrates. The experimental results showed that the I_D–V_G curves shifted toward a negative gate voltage as the concentration of proteinogenic amino acid in solution increased for all 20 types of proteinogenic amino acid. This indicates that the inherent mechanism of amino acid adsorption on graphene films is electron doping. In addition, these results help to elucidate the mechanism of protein adsorption onto epitaxial graphene FETs. Specifically, these phenomena demonstrate that non-specific protein binding always leads to electron doping of the graphene film.

See the supplementary material for additional information on the I_D–V_G characteristics of proteinogenic amino acids.

This work was supported by JSPS KAKENHI (Grant No. JP21H01394).

AUTHOR DECLARATIONS

Conflict of Interest

The authors have no conflicts to disclose.

Author Contributions

Sota Yamasaki: Validation (equal); Writing – original draft (lead); Writing – review & editing (equal). **Hiroki Nakai**: Validation (equal). **Keita Murayama**: Validation (equal). **Yasuhide Ohno**: Conceptualization (lead); Project administration (lead); Supervision (equal); Writing – review & editing (equal). **Masao Nagase**: Funding acquisition (lead); Supervision (equal); Writing – review & editing (equal).

DATA AVAILABILITY

The data that support the findings of this study are available from the corresponding author upon reasonable request.

REFERENCES

[1] G. Seo, G. Lee, M. J. Kim, S.-H. Baek, M. Choi, K. B. Ku, C.-S. Lee, S. Jun, D. Park, H. G. Kim, S.-J. Kim, J.-O. Lee, B. T. Kim, E. C. Park, and S. I. Kim, ACS Nano **14**(4), 5135–5142 (2020).
[2] A. Gao, N. Lu, Y. Wang, and T. Li, Sci. Rep. **6**, 22554 (2016).
[3] H. Chen, X. Zhao, Z. Xi, Y. Zhang, H. Li, Z. Li, H. Shi, L. Huang, R. Shen, J. Tao, and T. Wang, Int. J. Nanomed. **14**, 2985–2993 (2019).
[4] S.-K. Cho and W.-J. Cho, Sensors **21**(12), 4213 (2021).
[5] P. Y. Huang, C. S. Ruiz-Vargas, A. M. van der Zande, W. S. Whitney, M. P. Levendorf, J. W. Kevek, S. Garg, J. S. Alden, C. J. Hustedt, Y. Zhu, J. Park, P. L. McEuen, and D. A. Muller, Nature **469**(7330), 389–392 (2011).
[6] D. Gozzi, A. Latini, and M. Tomellini, J. Phys. Chem. C **113**(1), 45–53 (2009).
[7] J. Liu, X. Chen, Q. Wang, M. Xiao, D. Zhong, W. Sun, G. Zhang, and Z. Zhang, Nano Lett. **19**(3), 1437–1444 (2019).
[8] A. K. Geim and K. S. Novoselov, Nat. Mater. **6**(3), 183–191 (2007).
[9] K. S. Novoselov, A. K. Geim, S. V. Morozov, D. Jiang, M. I. Katsnelson, I. V. Grigorieva, S. V. Dubonos, and A. A. Firsov, Nature **438**(7065), 197–200 (2005).
[10] K. I. Bolotin, K. J. Sikes, Z. Jiang, M. Klima, G. Fudenberg, J. Hone, P. Kim, and H. L. Stormer, Solid State Commun. **146**(9–10), 351–355 (2008).
[11] C. N. R. Rao, K. Gopalakrishnan, and U. Maitra, ACS Appl. Mater. Interfaces **7**(15), 7809–7832 (2015).
[12] A. Purwidyantri, T. Domingues, J. Borme, J. R. Guerreiro, A. Ipatov, C. M. Abreu, M. Martins, P. Alpuim, and M. Prado, Biosensors **11**(1), 24 (2021).
[13] N. Kumar, M. Rana, M. Geiwitz, N. I. Khan, M. Catalano, J. C. Ortiz-Marquez, H. Kitadai, A. Weber, B. Dweik, X. Ling, T. van Opijnen, A. A. Argun, and K. S. Burch, ACS Nano **16**(3), 3704–3714 (2022).
[14] Y. Ohno, K. Maehashi, and K. Matsumoto, Biosens. Bioelectron. **26**(4), 1727–1730 (2010).
[15] L. Zhou, K. Wang, Z. Wu, H. Dong, H. Sun, X. Cheng, H. l. Zhang, H. Zhou, C. Jia, Q. Jin, H. Mao, J.-L. Coll, and J. Zhao, Langmuir **32**, 12623–12631 (2016).
[16] Z. Yan, Z. Peng, and J. M. Tour, Acc. Chem. Res. **47**(4), 1327–1337 (2014).
[17] A. Kumari, N. Prasad, P. K. Bhatnagar, P. C. Mathur, A. K. Yadav, C. V. Tomy, and C. S. Bhatia, Diamond Relat. Mater. **45**, 28–33 (2014).
[18] A. Pirkle, J. Chan, A. Venugopal, D. Hinojos, C. W. Magnuson, S. McDonnell, L. Colombo, E. M. Vogel, R. S. Ruoff, and R. M. Wallace, Appl. Phys. Lett. **99**(12), 122108 (2011).
[19] J. H. Jung, I. Y. Sohn, D. J. Kim, B. Y. Kim, M. Jang, and N.-E. Lee, Carbon **62**, 312–321 (2013).

[20]T. Aritsuki, T. Nakashima, K. Kobayashi, Y. Ohno, and M. Nagase, Jpn. J. Appl. Phys. **55**, 06GF03 (2016).
[21]S. Kim, H. Ryu, S. Tai, M. Pedowitz, J. R. Rzasa, D. J. Pennachio, J. R. Hajzus, D. K. Milton, R. Myers-Ward, and K. M. Daniels, Biosens. Bioelectron. **197**, 113803 (2022).
[22]T. Mitsuno, Y. Taniguchi, Y. Ohno, and M. Nagase, Appl. Phys. Lett. **111**(21), 213103 (2017).
[23]H. Nakai, D. Akiyama, Y. Taniguchi, I. Kishinobu, H. Wariishi, Y. Ohno, M. Nagase, T. Ikeda, A. Tabata, and H. Nagamune, J. Appl. Phys. **130**(7), 074502 (2021).
[24]C. N. Pace, H. Fu, K. L. Fryar, J. Landua, S. R. Trevino, B. A. Shirley, M. M. Hendricks, S. Iimura, K. Gajiwala, J. M. Scholtz, and G. R. Grimsley, J. Mol. Biol. **408**(3), 514–528 (2011).
[25]D. R. Davies and G. H. Cohen, Proc. Natl. Acad. Sci. U. S. A. **93**(1), 7–12 (1996).
[26]O. Leenaerts, B. Partoens, and F. M. Peeters, Phys. Rev. B **77**, 125416 (2008).
[27]M. B. Lerner, N. Kybert, R. Mendoza, R. Villechenon, M. A. Bonilla Lopez, and A. T. Charlie Johnson, Appl. Phys. Lett. **102**, 183113 (2013).
[28]M. B. Lerner, J. M. Resczenski, A. Amin, R. R. Johnson, J. I. Goldsmith, and A. T. C. Johnson, J. Am. Chem. Soc. **134**, 14318–14321 (2012).
[29]S. J. Rodríguez and E. A. Albanesi, Phys. Chem. Chem. Phys. **21**(2), 597–606 (2019).
[30]S. S. K. Mallineni, J. Shannahan, A. J. Raghavendra, A. M. Rao, J. M. Brown, and R. Podila, ACS Appl. Mater. Interfaces **8**(26), 16604–16611 (2016).
[31]S. Pandit and M. De, J. Phys. Chem. C **121**(1), 600–608 (2017).
[32]S. J. Rodríguez, L. Makinistian, and E. Albanesi, J. Comput. Electron. **16**(1), 127–132 (2017).
[33]Q. Gao, W. Xu, Y. Xu, D. Wu, Y. Sun, F. Deng, and W. Shen, J. Phys. Chem. B **112**(7), 2261–2267 (2008).
[34]C. Mathé, S. Devineau, J.-C. Aude, G. Lagniel, S. Chédin, V. Legros, M.-H. Mathon, J.-P. Renault, S. Pin, Y. Boulard, and J. Labarre, PLoS One **8**(11), e81346 (2013).
[35]D. Sebben and P. Pendleton, J. Chem. Thermodyn. **87**, 96 (2015).
[36]S. Tanabe, Y. Sekine, H. Kageshima, M. Nagase, and H. Hibino, Appl. Phys. Express **3**, 075102 (2010).
[37]M. T. Hwang, M. Heiranian, Y. Kim, S. You, J. Leem, A. Taqieddin, V. Faramarzi, Y. Jing, I. Park, A. M. van der Zande, S. Nam, N. R. Aluru, and R. Bashir, Nat. Commun. **11**(1), 1543 (2020).
[38]Y. Ohno, S. Okamoto, K. Maehashi, and K. Matsumoto, Jpn. J. Appl. Phys. **52**(11R), 110107 (2013).
[39]Y. Taniguchi, T. Miki, Y. Ohno, M. Nagase, Y. Arakawa, Y. Imada, K. Minagawa, and M. Yasuzawa, Jpn. J. Appl. Phys. **58**(5), 055001 (2019).
[40]J. Ping, R. Vishnubhotla, A. Vrudhula, and A. T. C. Johnson, ACS Nano **10**(9), 8700–8704 (2016).
[41]G. Wernke, M. Fernandes Silva, E. A. d. Silva, M. R. Fagundes-Klen, P. Y. R. Suzaki, C. C. Triques, and R. Bergamasco, Colloids Surf., A **627**, 127203 (2021).
[42]W. Qin, X. Li, W.-W. Bian, X.-J. Fan, and J.-Y. Qi, Biomaterials **31**(5), 1007–1016 (2010).